

Trajectory Optimization on Matrix Lie Groups with Differential Dynamic Programming and Nonlinear Constraints

Gokhan Alcan^a, Fares J. Abu-Dakka^b and Ville Kyrki^a

Abstract—Matrix Lie groups are an important class of manifolds commonly used in control and robotics, and the optimization of control policies on these manifolds is a fundamental problem. In this work, we propose a novel approach for trajectory optimization on matrix Lie groups using an augmented Lagrangian-based constrained discrete Differential Dynamic Programming. The method involves lifting the optimization problem to the Lie algebra in the backward pass and retracting back to the manifold in the forward pass. In contrast to previous approaches which only addressed constraint handling for specific classes of matrix Lie groups, the proposed method provides a general approach for nonlinear constraint handling for generic matrix Lie groups. We also demonstrate the effectiveness of the method in handling external disturbances through its application as a Lie-algebraic feedback control policy on SE(3). Experiments show that the approach is able to effectively handle configuration, velocity and input constraints and maintain stability in the presence of external disturbances.

Index Terms—Matrix Lie groups, Geometric control, Trajectory optimization, Differential Dynamic Programming, Constrained optimization.

I. INTRODUCTION

MANY physical systems such as robots have non-Euclidean configuration spaces. The use of local coordinates to model these spaces can result in various issues. One issue is that these coordinate systems may suffer from singularities or degeneracies, where the coordinates become ill-defined or degenerate. For example, Euler angles can experience gimbal lock, where two of the angles become degenerate, leading to a loss of a degree of freedom and making it difficult to represent certain configurations of the system [2], [1]. Similarly, quaternions can experience a similar loss of degree of freedom when their magnitude becomes close to zero and multiple different representations can describe the same configuration [3], although it has global representation. These types of singularities can make it difficult to accurately represent the transition between certain configurations of the system, and may require the use of additional techniques to avoid or mitigate these issues.

This work was supported by the Academy of Finland under Grants 345661 and 347199. Abu-Dakka, F. is supported by the European project euROBIN under grant agreement No 101070596.

Corresponding author: Gokhan Alcan (gokhan.alcan@aalto.fi)

^a Intelligent Robotics Group, Department of Electrical Engineering and Automation, Aalto University, 02150 Espoo, Finland.

^b Munich Institute of Robotics and Machine Intelligence, Technische Universität München, 80992 München, Germany. Part of the research presented in this work was conducted when F. Abu-Dakka was at Aalto University.

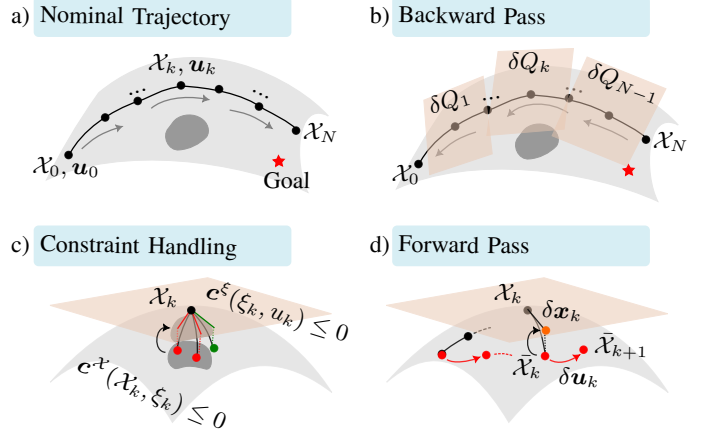


Fig. 1. Illustration of the proposed method. a) A trajectory on the configuration manifold is generated using a given nominal input sequence. b) The derivatives of the Q-function are calculated within local tangent spaces. c) The effects of configuration and velocity constraints are also included within local tangent space in the backward pass. d) The forward pass employs closed-loop control inputs to update control inputs. The updated trajectory is then used as the new nominal trajectory for the next iteration.

The geometry of configuration spaces can be effectively modeled through the use of matrix Lie groups, which provide a well-structured and continuous framework for comprehending the structure and motion of the underlying system [4], [5]. In recent years, geometric control techniques have gained considerable traction within the fields of robotics and control systems, as they seamlessly blend differential geometry and control theory [6], [7]. However, current approaches to solving geometric optimal control problems suffer from either reliance on specific problem details to simplify optimality conditions [8], [9] or growing complexities with the number of time instances [10], [11]. To overcome these limitations, Differential Dynamic Programming (DDP) has become a promising approach for numerically solving such problems. Nevertheless, existing DDP-based geometric control techniques have certain limitations, including explicit consideration of only specific matrix Lie groups [12], omission of state constraints [13], [14], [15], or handling of constraints limited to particular groups only [16].

In this paper, we develop a DDP-based geometric control method for matrix Lie groups that incorporates generic nonlinear constraints (Fig. 1) overcoming the aforementioned limitations. The main contributions of our work are:

- 1) Development of a novel augmented Lagrangian based constrained DDP algorithm for trajectory optimization on matrix Lie groups.
- 2) A principled approach for nonlinear constraint handling for generic matrix Lie groups. This approach overcomes the limitations in [16], which only addressed constraint handling for $SO(3)$ constraints.
- 3) Evaluating the effectiveness of the proposed DDP method in handling external disturbances through its application in a numerical simulation as a Lie-algebraic feedback control policy on $SE(3)$.

The rest of this paper is organized as follows. Section II discusses related works from classical control to constrained optimal control employed in smooth manifold systems. In Section III, we provide preliminaries regarding matrix Lie groups. Section IV defines the trajectory optimization problem for matrix Lie groups. We detail our proposed method in Section V. In Section VI, we provide numerical simulation experiments for $SE(3)$ to demonstrate the effectiveness of our approach. Finally, the paper is concluded with potential directions for future work in Section VII.

II. RELATED WORK

In recent years, there has been a significant effort to incorporate modern control theory into smooth manifold systems, resulting in a diverse range of theoretical outcomes including stability analysis, controllability, and feedback control design [6], [7]. As an early example, a classical PID-type controller has been successfully applied to fully actuated mechanical systems [6], utilizing configuration and velocity errors defined on a Riemannian manifold. More recently, researchers have developed locally exponentially stable geometric tracking controllers for Unmanned Aerial Vehicles (UAVs) by taking into account the dynamics of rigid bodies on $SO(3)$ [17] and $SE(3)$ [18]. Although these methods excel at point stabilization, they do not generate optimal trajectories and require predefined reference trajectories to achieve complex tasks.

Optimization-based control utilizing geometric methods aims to generate optimal trajectories on Riemannian manifolds. Bloch *et al.* [8] investigated a variational optimal control problem for a 3D rigid body representing dynamics on the Lie group $SO(3)$, while Kobilarov and Marsden [9] developed necessary conditions for optimal trajectories that correspond to discrete geodesics of a higher-order system and developed numerical methods for their computation. Saccon *et al.* [19] derived the projection operator framework on Lie groups, applying it to continuous-time trajectory-optimization problems, and Teng *et al.* [14] developed a geometric error-state Model Predictive Control (MPC) for tracking control of systems evolving on connected matrix Lie groups. Even though these methods consider dynamic and kinematic constraints, they lack the ability to account for generic state constraints such as obstacle avoidance.

In the trajectory optimization field, various studies have aimed to handle constraints in different ways. One of the most straightforward approaches is to formulate a nonlinear program that minimizes the cost function while satisfying all the

boundary conditions and constraints. Lee *et al.* [20] proposed a nonlinear MPC framework for spacecraft attitude control on the $SO(3)$ group, where they considered control and exclusion zone constraints. Similarly, Hong *et al.* [21] combined the Gauss-Newton method with a proximal operator to handle inequality constraints for trajectory optimization on $SO(3)$. Some researchers have focused on optimizing trajectories on other matrix Lie groups, including Kalabic *et al.* [22], who designed MPC on $SE(3)$ by considering only boundary constraints for states and inputs, and Ding *et al.* [23], who proposed a representation-free MPC for the $SE(3)$ group. However, these methods have limitations, such as being restricted to specific matrix Lie groups and increasing complexity with the number of time instances. Recently, Watterson *et al.* [24] proposed a graph search-based safe corridor on manifolds method to optimize trajectories on a Riemannian manifold with obstacles. Although successful in some robotic applications, the method's sensitivity to parameterization affects optimality performance and computational cost.

Different from the aforementioned MPC based direct methods, DDP is an indirect numerical method for solving optimal control problems through optimizing the control inputs. Originally proposed by Mayne and Jacobson [25], DDP has been applied to a wide range of complex, high-dimensional systems [26]. One of the key advantages of DDP is its scalability, which allows it to handle large and complex systems with many degrees of freedom. In addition, DDP has a fast convergence rate, which allows it to quickly find near-optimal solutions to the control problem. Another important attribute of DDP is its ability to generate feedback control policies, which can be used to implement the optimal control solution in real-time.

Several early works have investigated the use of DDP for geometric control [12], [27]. These studies focused on specific matrix Lie groups, including $SE(3)$, in order to derive the final form of the DDP algorithm for applications in geometric control. Boutselis and Theodorou [13] extended the original DDP method by using quadratic expansion schemes for cost functions and dynamics defined on Lie groups. They demonstrated that DDP has significantly better convergence rates compared to Sequential Quadratic Programming (SQP) methods. Teng *et al.* [15] further improved the convergence performance of DDP for matrix groups by designing the control objective in its Lie algebra. Both of these approaches [13], [15] formulate the trajectory optimization on matrix Lie groups in an unconstrained framework. In order to address this limitation, Liu *et al.* [16] extended the work [13] by imposing $SO(3)$ constraints. However, this method is not generalizable to nonlinear constraints for generic matrix Lie groups. This paper aims to solve the problem of handling generic constraints by extending the idea of Lie algebraic cost definition [15] and developing a DDP method for matrix Lie groups under nonlinear constraints.

III. PRELIMINARIES

Consider \mathcal{G} is an n -dimensional matrix Lie group, and \mathfrak{g} its associated Lie algebra, i.e., its tangent space at the identity.

Isomorphism between the vector space \mathbb{R}^n and \mathfrak{g} can be defined through the following operators:

$$\begin{aligned} (\cdot)^\wedge : \mathbb{R}^n &\mapsto \mathfrak{g} \\ (\cdot)^\vee : \mathfrak{g} &\mapsto \mathbb{R}^n. \end{aligned} \quad (1)$$

Mapping between \mathbb{R}^n and \mathcal{G} can be defined using the functions $\text{Exp}(\cdot) : \mathbb{R}^n \mapsto \mathcal{G}$ and $\text{Log}(\cdot) : \mathcal{G} \mapsto \mathbb{R}^n$ for any $\phi \in \mathbb{R}^n$ and $\mathcal{X} \in \mathcal{G}$ as follows:

$$\begin{aligned} \text{Exp}(\phi) &= \text{expm}(\phi^\wedge) = \mathcal{X} \\ \text{Log}(\mathcal{X}) &= \text{logm}(\mathcal{X})^\vee = \phi \end{aligned} \quad (2)$$

where $\text{expm}(\cdot)$ and $\text{logm}(\cdot)$ are the matrix exponential and logarithm, respectively.

The adjoint action, denoted as $\text{Ad}_{\mathcal{X}} : \mathfrak{g} \mapsto \mathfrak{g}$ for any $\mathcal{X} \in \mathcal{G}$, is a Lie algebra isomorphism that allows change of frames. Given $\phi, \eta \in \mathbb{R}^n$ and $\phi^\wedge, \eta^\wedge \in \mathfrak{g}$, the adjoint action can be expressed in the function form as

$$\text{Ad}_{\mathcal{X}}(\phi) = \mathcal{X}\phi^\wedge\mathcal{X}^{-1} \quad (3)$$

or in the matrix form as

$$(\text{Ad}_{\mathcal{X}}\phi)^\wedge = \mathcal{X}\phi^\wedge\mathcal{X}^{-1}. \quad (4)$$

The adjoint map is the derivative of the adjoint action with respect to \mathcal{X} at the identity element and is defined as

$$\text{ad}_\phi\eta = [\phi^\wedge, \eta^\wedge] \quad (5)$$

where $[\phi^\wedge, \eta^\wedge]$ is the Lie bracket, defined as

$$[\phi^\wedge, \eta^\wedge] = \phi^\wedge\eta^\wedge - \eta^\wedge\phi^\wedge. \quad (6)$$

IV. PROBLEM DEFINITION

We consider systems whose states reside in the tangent bundle of a matrix Lie group. This encompasses a diverse array of systems [9] whose states can be represented as pairs $\{\mathcal{X}, \xi^\wedge\} \in \mathcal{G} \times \mathfrak{g}$, where \mathcal{X} represents a configuration and ξ^\wedge represents the velocity (rate of change) of that configuration. The continuous-time equations of motion for such systems can be written as:

$$\begin{aligned} \dot{\mathcal{X}}_t &= \mathcal{X}_t \xi_t^\wedge \\ \dot{\xi}_t &= f(\xi_t, u_t) \end{aligned} \quad (7)$$

where $u_t \in \mathbb{R}^m$ is the generalized control input and $f(\cdot)$ is the function of velocity dynamics. For a given initial state $\{\mathcal{X}_0, \xi_0\}$, a goal state $\{\mathcal{X}_g, \xi_g\}$, and a time horizon N , we define the discrete-time constrained optimal control problem as

$$\begin{aligned} \min_{u_0, \dots, u_{N-1}} \quad & \ell^f(\mathcal{X}_N, \xi_N) + \sum_{k=0}^{N-1} \ell(\mathcal{X}_k, \xi_k, u_k) \\ \text{subject to} \quad & \mathcal{X}_{k+1} = F_{\mathcal{X}}(\mathcal{X}_k, \xi_k), \quad k = 0, \dots, N-1 \\ & \xi_{k+1} = F_{\xi}(\xi_k, u_k), \quad k = 0, \dots, N-1 \\ & u_{\min} \leq u_k \leq u_{\max}, \quad \forall k, \\ & \mathbf{g}(\mathcal{X}_k, \xi_k, u_k) \leq \mathbf{0}, \quad \forall k, \\ \text{given} \quad & \mathcal{X}_0, \xi_0, \end{aligned} \quad (8)$$

where $\ell^f : \mathcal{G} \times \mathbb{R}^n \mapsto \mathbb{R}$ and $\ell : \mathcal{G} \times \mathbb{R}^n \times \mathbb{R}^m \mapsto \mathbb{R}$ are the final cost and the running cost, respectively. $F_{\mathcal{X}}$ and F_{ξ} are the

discretized form of the configuration and velocity dynamics, which can be obtained by using a zero-order hold or first-order Euler integration method with a fixed time step Δt . Lastly, \mathbf{g} is a vector of p constraints in the form of differentiable nonlinear functions representing the state constraints.

V. PROPOSED METHOD

The analytic solution of the general problem outlined in Section IV is often difficult. Additionally, finding the global minimum numerically can be time-consuming, particularly for systems with high dimensions. Therefore, we propose a method that finds feasible solutions, even if they may not be globally optimal. To accomplish this, we utilize the DDP framework [25], which iteratively solves sub-optimization problems in the backward pass and generates a new trajectory in the forward pass based on the found optimal policy, in order to approach a local optimum.

To account for constraints imposed on the system, whose states lie in the tangent bundle of a matrix Lie group, we optimize an augmented Lagrangian function that combines trajectory cost with constraint penalties. The approach involves lifting the problem to the Lie algebra in the backward pass by computing the gradient of the cost function within the corresponding Lie algebra, and retracting back to the manifold in the forward pass by integrating the dynamics using the optimal policy obtained in the backward pass.

A. Dynamics on Tangent Space

The central concept of DDP is that, at each iteration, all nonlinear constraints and objectives are approximated using first or second-order Taylor series expansions. This allows the approximate functions, which now operate on deviations from the nominal trajectory, to be solved using discrete Linear-Quadratic Regulator (LQR) techniques. In order to define the cost and constraint functions in Lie algebra, we need to determine the error dynamics for the configuration. To obtain the perturbed state dynamics, we followed the approach proposed by Teng *et al.* [14]. For completeness, we outline the necessary steps here. Interested readers may refer to [14], [15] for more information.

Consider a perturbed state $\{\mathcal{X}_p, \xi_p^\wedge\}$ that is in the vicinity of a nominal state $\{\mathcal{X}, \xi^\wedge\}$. Then, the configuration error Ψ can be defined as

$$\Psi = \mathcal{X}^{-1}\mathcal{X}_p \in \mathcal{G}. \quad (9)$$

Differentiating both sides of (9) yields the configuration error dynamics as

$$\begin{aligned} \dot{\Psi} &= \mathcal{X}^{-1} \frac{d}{dt}(\mathcal{X}_p) + \frac{d}{dt}(\mathcal{X}^{-1})\mathcal{X}_p \\ &= \mathcal{X}^{-1}\dot{\mathcal{X}}_p - \mathcal{X}^{-1}\dot{\mathcal{X}}\mathcal{X}^{-1}\mathcal{X}_p \\ &= \mathcal{X}^{-1}\mathcal{X}_p\xi_p^\wedge - \mathcal{X}^{-1}\mathcal{X}\xi^\wedge\mathcal{X}^{-1}\mathcal{X}_p \\ &= \Psi\xi_p^\wedge - \xi^\wedge\Psi. \end{aligned} \quad (10)$$

Here, we can define a vector ψ in \mathbb{R}^n such that the matrix exponential of ψ^\wedge corresponds to Ψ , denoted as $\Psi = \text{expm}(\psi^\wedge)$. Using the first-order approximation of the matrix exponential,

which states that $\expm(\psi^\wedge) \approx I_n + \psi^\wedge$, the dynamics of the configuration error in (10) can be linearized as follows:

$$\begin{aligned}
\dot{\Psi} &= \Psi \xi_p^\wedge - \xi^\wedge \Psi \\
&= (I_n + \psi^\wedge) \xi_p^\wedge - \xi^\wedge (I_n + \psi^\wedge) \\
&= \xi_p^\wedge + \psi^\wedge \xi_p^\wedge - \xi^\wedge - \xi^\wedge \psi^\wedge \\
&= \xi_p^\wedge - \xi^\wedge + \psi^\wedge \xi_p^\wedge - \xi^\wedge \psi^\wedge \\
&= \xi_p^\wedge - \xi^\wedge + \psi^\wedge (\xi^\wedge - \xi^\wedge + \xi_p^\wedge) - \xi^\wedge \psi^\wedge \\
&= \xi_p^\wedge - \xi^\wedge + \psi^\wedge \xi^\wedge - \xi^\wedge \psi^\wedge + \psi^\wedge (\xi_p^\wedge - \xi^\wedge) \\
&= \xi_p^\wedge - \xi^\wedge + \psi^\wedge \xi^\wedge - \xi^\wedge \psi^\wedge \\
&= \xi_p^\wedge - \xi^\wedge + \text{ad}_\psi \xi \\
\dot{\psi} &= \xi_p^\wedge - \xi^\wedge - \text{ad}_\xi \psi
\end{aligned} \tag{11}$$

Note that the second order term of $\psi^\wedge (\xi_p^\wedge - \xi^\wedge)$ is also discarded to obtain the linear dynamics of the configuration error [14], [15]. ψ in (11) is the perturbed configuration represented in Lie algebra. The perturbed velocity and control input are also defined as

$$\delta \xi = \xi_p - \xi, \quad \text{and} \quad \delta u = u_p - u \tag{12}$$

The perturbed velocity dynamics then become:

$$\dot{\delta \xi}_t = \mathbf{\Gamma}_t \delta \xi_t + \mathbf{\Lambda}_t \delta u_t \tag{13}$$

where $\mathbf{\Gamma}_t$ and $\mathbf{\Lambda}_t$ are the Jacobians of $f(\xi_t, u_t)$ defined in (7) around the nominal trajectory about ξ_t and u_t .

Defining the perturbed states as concatenation

$$\mathbf{x} = \begin{bmatrix} \psi \\ \delta \xi \end{bmatrix}, \quad \bar{\mathbf{u}} = \delta u \tag{14}$$

the perturbed state dynamics can be expressed as

$$\begin{aligned}
\dot{\mathbf{x}} &= h(\mathbf{x}, \mathbf{u}) \\
\dot{\mathbf{x}} &= \underbrace{\begin{bmatrix} -\text{ad}_\xi & I_n \\ \mathbf{0}_{n \times n} & \mathbf{\Gamma}_t \end{bmatrix}}_{\triangleq \mathbf{A}_t} \mathbf{x} + \underbrace{\begin{bmatrix} \mathbf{0}_{n \times m} \\ \mathbf{\Lambda}_t \end{bmatrix}}_{\triangleq \mathbf{B}_t} \bar{\mathbf{u}}
\end{aligned} \tag{15}$$

The discretized versions of the matrices \mathbf{A}_t and \mathbf{B}_t can be simply obtained by applying a zero-order hold or a first-order Euler integration method with a fixed time step Δt .

B. Constraint Handling

In order to handle the constraints in DDP framework, we need their first-order approximations around the perturbed state dynamics introduced in (15) as follows:

$$\begin{aligned}
\bar{\mathbf{c}}(\mathbf{x} + \delta \mathbf{x}, \mathbf{u} + \delta \mathbf{u}) &\approx \bar{\mathbf{c}}(\mathbf{x}, \mathbf{u}) \\
&\quad + \bar{\mathbf{c}}_{\mathbf{x}}(\mathbf{x}, \mathbf{u}) \delta \mathbf{x} + \bar{\mathbf{c}}_{\mathbf{u}}(\mathbf{x}, \mathbf{u}) \delta \mathbf{u}
\end{aligned} \tag{16}$$

where

$$\bar{\mathbf{c}}(\mathbf{x}) = \begin{bmatrix} \bar{\mathbf{c}}^{\mathcal{X}}(\psi^c) \\ \bar{\mathbf{c}}^\xi(\delta \xi^b) \end{bmatrix} \tag{17}$$

$\bar{\mathbf{c}}_{\mathbf{x}}$ and $\bar{\mathbf{c}}_{\mathbf{u}}$ are the derivative of $\bar{\mathbf{c}}$ with respect to \mathbf{x} and \mathbf{u} , respectively. By first-order approximation, we consider the constraints in vector $\mathbf{g}(\mathcal{X}_k, \xi_k, u_k)$ in (8) as two types: those

that constrain the velocity and those that specify configurations to be avoided. This allows us to separately handle the constraints on velocity (\mathbf{c}_ξ) and on configuration ($\mathbf{c}_{\mathcal{X}}$) as

$$\begin{aligned}
\mathbf{c}^\xi(\xi_k, u_k) &\leq 0 \\
\mathbf{c}^{\mathcal{X}}(\mathcal{X}_k, \xi_k) &\leq 0
\end{aligned} \tag{18}$$

The velocity component of the state (ξ) resides in \mathbb{R}^n , and as a result, constraints involving any metric in Euclidean space produce a distance vector in \mathbb{R}^n . Therefore, any boundary velocity constraint can be written as

$$\delta \xi^b = \xi_b - \xi, \quad \bar{\mathbf{c}}^\xi(\beta \delta \xi^b) \leq 0 \tag{19}$$

where

$$\beta = \begin{cases} -1 & \text{if } \xi^b \text{ is upper bound,} \\ +1 & \text{if } \xi^b \text{ is lower bound} \end{cases} \tag{20}$$

On the other hand, the difference between two group elements in the configuration state produces a geodesic in the group. To handle this, we propose mapping the distance geodesic to the tangent space of the configuration at the current time step and addressing the constraint in that vector space.

Configuration avoidance constraints can typically be formulated as inequality constraints using an n-spherical function, with the center of the n-sphere located at the configuration to be avoided (\mathcal{X}_c) and the radius (r_c) defining the restricted region. This allows us to specify a region of configurations that should be avoided. The distance between the nominal and restricted configurations in the tangent space of the nominal trajectory, ψ^c , is given by:

$$\psi^c = \text{logm}(\mathcal{X}^{-1} \mathcal{X}_c) \tag{21}$$

Then, the configuration avoidance constraint can be written as

$$\bar{\mathbf{c}}^{\mathcal{X}}(\psi^c) = (r_c^2 - \|\psi^c\|_2) \leq 0 \tag{22}$$

In this approach, we consider the same restricted region for each axis in the n-dimensional sphere. However, it is also possible to specify different radius values for each axis, resulting in an n-dimensional ellipsoid as the restricted region. Our method can accommodate these types of configuration constraints as well.

If the constraints are designed according to equations (19) and (22), the derivatives can be calculated as follows:

$$\begin{aligned}
\bar{\mathbf{c}}_{\mathbf{x}}(\mathbf{x}, \mathbf{u}) &= \begin{bmatrix} -2(\text{ad}_\xi \psi^c)^\top & 2\psi^{c\top} \\ \mathbf{0}_{1 \times n} & \beta(\mathbf{\Gamma} \delta \xi^b)^\top \end{bmatrix} \\
\bar{\mathbf{c}}_{\mathbf{u}}(\mathbf{x}, \mathbf{u}) &= \begin{bmatrix} \mathbf{0}_{1 \times m} \\ \beta(\mathbf{\Lambda}^\top \delta \xi^b)^\top \end{bmatrix}
\end{aligned} \tag{23}$$

C. Constrained Differential Dynamic Programming

Using the perturbed state dynamics defined in (15), the backward pass of DDP is lifted to the tangent space. The backward pass of DDP involves computing the cost-to-go function at each time step in a given trajectory. Unlike [15], the proposed algorithm not only considers the objective function when calculating the cost-to-go function, but also takes into account any constraints on the state and control variables.

An effective method for solving constrained optimization problems is to transform the constraints into the objective

function and iteratively increase the penalty for violating or approaching them. This technique, known as the penalty method, guarantees convergence to the optimal solution as the penalty terms increase indefinitely. However, this may not be practical to implement in numerical optimization routines due to the limitations of finite precision arithmetic. Augmented Lagrangian methods [29] offer an alternative solution by maintaining estimates of the Lagrange multipliers associated with the constraints, allowing for convergence to the optimal solution without requiring the penalty terms to increase indefinitely. Here we obtain the augmented Lagrangian as

$$\begin{aligned}\mathcal{L}_A &= \mathcal{L}_N(\mathbf{x}_N) + \sum_{k=0}^{N-1} \mathcal{L}_k(\mathbf{x}_k, \mathbf{u}_k) \\ \mathcal{L}_N(\mathbf{x}_N) &= \bar{\ell}^f(\mathbf{x}_N) + (\lambda + \frac{1}{2}\bar{\mathbf{g}}(\mathbf{x}_N)I_\mu)^\top \bar{\mathbf{g}}(\mathbf{x}_N) \\ \mathcal{L}_k(\mathbf{x}_k, \mathbf{u}_k) &= \bar{\ell}(\mathbf{x}_k, \mathbf{u}_k) + (\lambda + \frac{1}{2}\bar{\mathbf{g}}(\mathbf{x}_k, \mathbf{u}_k)I_\mu)^\top \bar{\mathbf{g}}(\mathbf{x}_k, \mathbf{u}_k)\end{aligned}\quad (24)$$

where $\bar{\ell}^f: \mathbb{R}^{2n} \mapsto \mathbb{R}$ and $\bar{\ell}: \mathbb{R}^{2n} \times \mathbb{R}^m \mapsto \mathbb{R}$ are the final cost and the running cost functions for perturbed system dynamics, respectively. A typical design of such functions is quadratic,

$$\begin{aligned}\bar{\ell}^f(\mathbf{x}) &= \frac{1}{2}\|\delta\mathbf{x}\|_{S_V}^2 \\ \bar{\ell}(\mathbf{x}, \mathbf{u}) &= \frac{1}{2}\|\delta\mathbf{x}\|_{S_Q}^2 + \frac{1}{2}\|\delta\mathbf{u}\|_{S_U}^2,\end{aligned}\quad (25)$$

where $S_V \in \mathbb{R}^{2n \times 2n}$, $S_Q \in \mathbb{R}^{2n \times 2n}$ and $S_U \in \mathbb{R}^{m \times m}$ are cost matrices that are specified by the user and remain constant.

In (24), $\bar{\mathbf{g}}$ is a vector of p constraints for perturbed state dynamics as introduced in (16). $\lambda \in \mathbb{R}^p$ is a Lagrange multiplier, $\mu \in \mathbb{R}^p$ is a penalty weight and $I_\mu \in \mathbb{R}^{p \times p}$ is the penalty matrix defined as

$$I_\mu = \begin{cases} 0 & \text{if } \mathbf{g}_i(\cdot) < 0 \text{ and } \lambda_i = 0, \\ \mu_i & \text{otherwise} \end{cases}\quad (26)$$

In general, one can define time-varying Lagrange multiplier and penalty weight, but we kept them constant for each time step within the same iteration for simplicity.

We define the cost-to-go and action-value functions V and Q as

$$\begin{aligned}V_k(\mathbf{x}_k) &= \min_{\mathbf{u}_k} \{\mathcal{L}_k(\mathbf{x}_k, \mathbf{u}_k)\} + V_{k+1}(\mathbf{A}_k\mathbf{x}_k + \mathbf{B}_k\mathbf{u}_k) \\ &= \min_{\mathbf{u}_k} Q(\mathbf{x}_k, \mathbf{u}_k).\end{aligned}\quad (27)$$

The matrices \mathbf{A}_k and \mathbf{B}_k represent the discretized versions of \mathbf{A}_t and \mathbf{B}_t in equation (15). A second-order Taylor series expansion of the cost-to-go function can be written

$$\delta V_k(x) \approx \frac{1}{2}\delta\mathbf{x}_k^\top V_{xx,k}\delta\mathbf{x}_k + V_{x,k}^\top\delta\mathbf{x}_k\quad (28)$$

where $V_{xx,k}$ and $V_{x,k}$ are the Hessian and gradient of the cost-to-go at time step k , respectively. The action-value function defined in (27) can be also approximated as a quadratic function as

$$\begin{aligned}Q(\mathbf{x} + \delta\mathbf{x}, \mathbf{u} + \delta\mathbf{u}) &\approx Q(\mathbf{x}, \mathbf{u}) + Q_x^\top\delta\mathbf{x} + Q_u^\top\delta\mathbf{u} \\ &\quad + \frac{1}{2}(\delta\mathbf{x}^\top Q_{xx}\delta\mathbf{x} + \delta\mathbf{u}^\top Q_{uu}\delta\mathbf{u}) \\ &\quad + \delta\mathbf{x}^\top Q_{xu}\delta\mathbf{u}.\end{aligned}\quad (29)$$

To compute the derivative matrices in (29):

$$\begin{aligned}Q_x &= \bar{\ell}_x + \mathbf{A}^\top V_x' + \bar{\mathbf{g}}_x^\top(\lambda + I_\mu\bar{\mathbf{g}}) \\ Q_u &= \bar{\ell}_u + \mathbf{B}^\top V_x' + \bar{\mathbf{g}}_u^\top(\lambda + I_\mu\bar{\mathbf{g}}) \\ Q_{xx} &= \bar{\ell}_{xx} + \mathbf{A}^\top V_{xx}'\mathbf{A} + \bar{\mathbf{g}}_x^\top I_\mu\bar{\mathbf{g}}_x + (V_x' h_{xx}) \\ Q_{uu} &= \bar{\ell}_{uu} + \mathbf{B}^\top V_{xx}'\mathbf{B} + \bar{\mathbf{g}}_u^\top I_\mu\bar{\mathbf{g}}_u + (V_x' h_{uu}) \\ Q_{ux} &= \bar{\ell}_{ux} + \mathbf{B}^\top V_{xx}'\mathbf{A} + \bar{\mathbf{g}}_u^\top I_\mu\bar{\mathbf{g}}_x + (V_x' h_{ux})\end{aligned}\quad (30)$$

To simplify the notation, we have omitted the time indices on all variables. All variables in this expression are evaluated at time step k , except for those marked with $'$, which are evaluated at time step $k+1$.

Calculating the full second-order expansion of the state dynamics (h_{xx} , h_{uu} , h_{ux}), can be computationally expensive, particularly for systems with complex dynamics and high-dimensional states. Discarding the second-order dynamics and computing only the first-order expansion result in a Gauss-Newton approximation of the true Hessian, which reduces the local fidelity and increases the number of iterations for convergence. However, these iterations are less expensive to compute which often leads to a shorter overall convergence time. Therefore, in this work, we eliminated the second-order dynamics as approximating the perturbed state dynamics as described in (11).

Minimizing (29) with respect to $\delta\mathbf{u}$ results in an affine controller

$$\delta\mathbf{u}^* = -Q_{uu}^{-1}(Q_{ux}\delta\mathbf{x} + Q_u) \triangleq \mathbf{K}\delta\mathbf{x} + \mathbf{d}\quad (31)$$

Substituting $\delta\mathbf{u}^*$ into (29) yields the derivatives of the cost-to-go at time step k in terms of the derivatives of the action value function as:

$$\begin{aligned}V_x &= Q_x + \mathbf{K}Q_u + \mathbf{K}^\top Q_{uu}\mathbf{d} + Q_{ux}^\top\mathbf{d}, \\ V_{xx} &= Q_{xx} + \mathbf{K}^\top Q_{uu}\mathbf{K} + \mathbf{K}^\top Q_{ux} + Q_{ux}^\top\mathbf{K}\end{aligned}\quad (32)$$

At the final step, V_x and V_{xx} can be easily computed as the first and second derivatives of the final cost function ($\bar{\ell}^f$). This way, the derivatives of the action-value function (30) and in turn the local optimal control policy (31) at each step can be calculated backward starting from the final step. After determining the optimal control policy for each time step, we update the nominal trajectories by simulating the dynamics forward on the manifold itself starting from the initial state as:

$$\delta\mathbf{x}_k = \begin{bmatrix} \logm(\mathcal{X}_k^{-1}\bar{\mathcal{X}}_k) \\ \bar{\xi}_k - \xi_k \end{bmatrix}\quad (33)$$

$$\begin{aligned}\delta\mathbf{u}_k &= \mathbf{K}_k\delta\mathbf{x}_k + \alpha\mathbf{d}_k \\ \bar{\mathbf{u}}_k &= \mathbf{u}_k + \delta\mathbf{u}_k\end{aligned}\quad (34)$$

$$\begin{aligned}\bar{\xi}_{k+1} &= \bar{\xi}_k + f(\xi, \bar{\mathbf{u}}_k)\Delta t \\ \bar{\mathcal{X}}_{k+1} &= \bar{\mathcal{X}}_k \expm(\bar{\xi}_{k+1}\Delta t)\end{aligned}\quad (35)$$

where $\{\mathcal{X}_k, \xi_k, u_k\}$ and $\{\bar{\mathcal{X}}_k, \bar{\xi}_k, \bar{u}_k\}$ represent the nominal state-actions and the updated state-actions at time step k , respectively. In (34), $0 \leq \alpha \leq 1$ is a scaling term for a simple linear search on the feedforward term. Practically, the parameter α is initially set to 1, but if the cost of the updated trajectory does not decrease, α will be decreased. Once the cost of the updated trajectory decreases, the forward

pass is successfully completed, the new trajectory is accepted as a nominal trajectory and the backward pass is triggered (Algorithm 1).

Algorithm 1: Constrained DDP for Matrix Lie Groups

```

1 Init:  $N, \mathcal{L}_A^-, tol, \rho, \lambda, \mu, \mathcal{X}_0, \xi_0, \mathcal{X}_g, \xi_g, \mathbf{u}_0, \dots, \mathbf{u}_{N-1}$ 
2 Calculate:  $\mathcal{X}_{1, \dots, N}, \xi_{1, \dots, N}$  integrating (7)
3 Calculate:  $\mathcal{L}_A$  using  $\{\mathcal{X}_k, \xi_k, \mathbf{u}_{k-1}\}_{k=1, \dots, N}$  (24)
4 while  $|\mathcal{L}_A - \mathcal{L}_A^-| > tol$  do
5   function Backward_Pass
6      $V_x(\mathbf{x}_N), V_{xx}(\mathbf{x}_N) \leftarrow \frac{\partial \mathcal{L}_N}{\partial \mathbf{x}}(\mathbf{x}_N), \frac{\partial^2 \mathcal{L}_N}{\partial \mathbf{x}^2}(\mathbf{x}_N)$ 
7     for  $k = N - 1, \dots, 0$  do
8       Calculate the derivatives of constraints
9        $\bar{\mathbf{c}}_x, \bar{\mathbf{c}}_u$  in local tangent space (23)
10      Calculate the derivatives of running cost
11       $\bar{\ell}_x, \bar{\ell}_u, \bar{\ell}_{ux}, \bar{\ell}_{xx}, \bar{\ell}_{uu}$ 
12      Calculate the derivatives of  $Q$  (30)
13      if  $Q_{uu} > 0$  then
14        Calculate  $K, d$  using  $Q_{uu}, Q_{xu}, Q_u$ 
15      else
16        Increase  $\rho$ 
17         $Q_{uu} \leftarrow Q_{uu} + \rho I$ 
18        Go to line 7
19   Reset  $\rho$ 
20   Init  $\alpha = 1$ 
21   function Forward_Pass
22      $\bar{\mathcal{X}}_0, \bar{\xi}_0 \leftarrow \mathcal{X}_0, \xi_0$ 
23     for  $k = 0, \dots, N - 1$  do
24       Calculate  $\delta \mathbf{x}_k$  in local tangent space (33)
25       Calculate updated input  $\bar{\mathbf{u}}_k$  (34)
26       Calculate  $\bar{\mathcal{X}}_{k+1}, \bar{\xi}_{k+1}$  on manifold (35)
27     Calculate  $\bar{\mathcal{L}}_A$  using  $\{\bar{\mathcal{X}}_k, \bar{\xi}_k, \bar{\mathbf{u}}_{k-1}\}_{k=1, \dots, N}$  (24)
28     if  $(\bar{\mathcal{L}}_A - \mathcal{L}_A) > 0$  then
29       Reduce  $\alpha$  and Go to line 20
30     else
31        $\mathcal{L}_A^- \leftarrow \mathcal{L}_A$ 
32        $\mathcal{L}_A \leftarrow \bar{\mathcal{L}}_A$ 
33        $\mathbf{u}_0, \dots, \mathbf{u}_{N-1} \leftarrow \bar{\mathbf{u}}_0, \dots, \bar{\mathbf{u}}_{N-1}$ 
34        $\xi_{1, \dots, N} \leftarrow \bar{\xi}_{1, \dots, N}$ 
35        $\mathcal{X}_{1, \dots, N} \leftarrow \bar{\mathcal{X}}_{1, \dots, N}$ 

```

To optimize the performance of DDP-based algorithms, there are a few implementation practices to consider. In the backward pass, Q_{uu} may need to be regularized as $Q_{uu} + \rho I$ if it is invertible or the former forward pass is unsuccessful, i.e., the cost does not decrease. Once the DDP iterations have converged for a given set of constraint parameters λ and μ , they can be updated using the following equations:

$$\begin{aligned} \lambda^+ &= \max(0, \lambda_i + \mu_i \bar{g}_i(\mathbf{x}^*, \mathbf{u}^*)) \\ \mu^+ &= \gamma \mu, \quad \gamma > 0 \end{aligned} \quad (36)$$

The DDP iterations can then be restarted again until convergence is achieved. For more information, see reference [29].

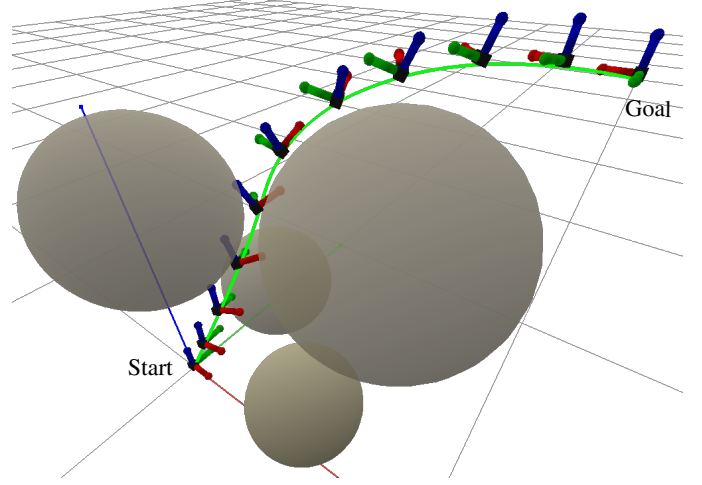


Fig. 2. The proposed constrained DDP method effectively optimizes the trajectory for an SE(3) object, taking into account both position and orientation constraints.

VI. EXPERIMENTS

The proposed method is employed here to optimize the trajectory of a system, whose states lie in the tangent bundle of a matrix Lie group. In order to demonstrate the effectiveness of our algorithm, we employ it for optimizing the trajectory of a mechanical system characterized by rigid body dynamics in SE(3) (Fig. 2), encompassing a broad range of robotics applications [14], [30].

A. Dynamics on SE(3)

We consider a 3D rigid body in SE(3) where the states of the system can be represented by a rotation matrix

$$R \in \text{SO}(3) \equiv \{R \in \mathbb{R}^{3 \times 3} | R^T R = I_3, \det(R) = 1\} \quad (37)$$

and position $p \in \mathbb{R}^3$. The homogeneous representation of a typical group element in SE(3) is

$$\mathcal{X} = \begin{bmatrix} R & p \\ 0 & 1 \end{bmatrix} \in \text{SE}(3) \quad (38)$$

The velocity vector ξ in SE(3) is known as a “twist” and is composed of both angular (ω) and linear (v) velocities in body frame as

$$\xi = \begin{bmatrix} \omega \\ v \end{bmatrix} \in \mathbb{R}^6, \quad \xi^\wedge = \begin{bmatrix} \omega^\wedge & v \\ 0 & 0 \end{bmatrix} \in \mathfrak{se}(3) \quad (39)$$

The forced Euler-Poincaré equations [28] define the twist dynamics as

$$J_b \dot{\xi} = \text{ad}_\xi^* J_b \xi + u \quad (40)$$

In this expression, J_b represents the generalized inertia matrix in the body fixed principal axes, while $u \in \mathfrak{g}^*$ represents the generalized control inputs including torques and forces (u_τ and u_f) applied to these axes. \mathfrak{g}^* denotes the cotangent space and the coadjoint map is represented by ad_ξ^* . The matrix representations of the adjoint action in the Lie algebra (ad_ξ) and the coadjoint map (ad_ξ^*) are as follows:

$$\text{ad}_\xi = \begin{bmatrix} \omega^\wedge & 0 \\ v^\wedge & \omega^\wedge \end{bmatrix}, \quad \text{ad}_\xi^* = \text{ad}_\xi^\top = - \begin{bmatrix} \omega^\wedge & v^\wedge \\ 0 & \omega^\wedge \end{bmatrix}. \quad (41)$$

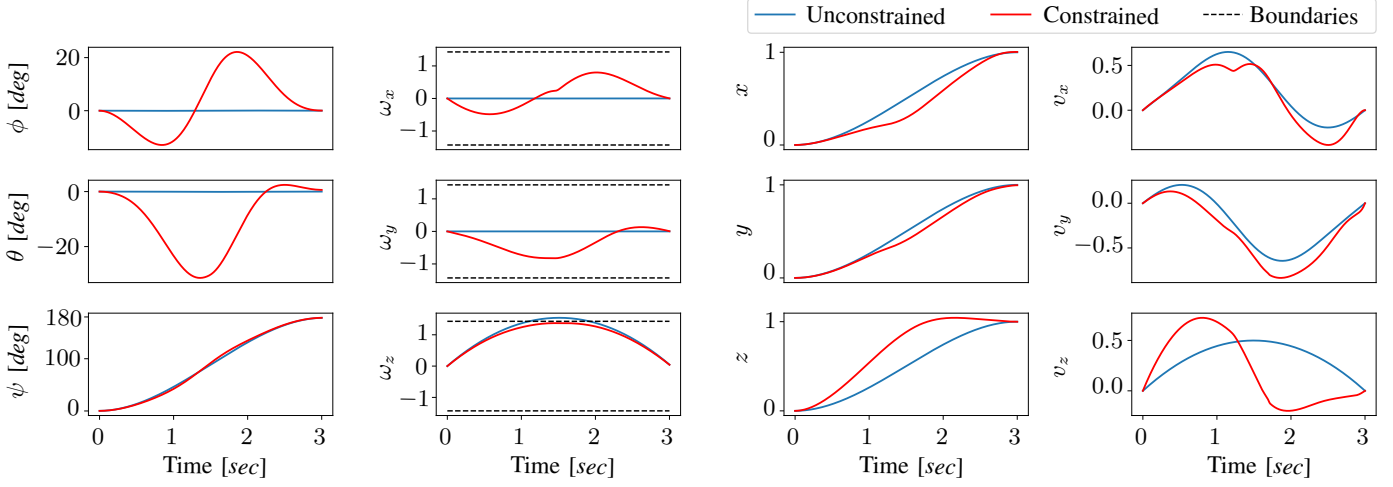


Fig. 3. Comparison of state trajectories generated by constrained and unconstrained DDP.

The continuous equations of motion described in (7) can be written for SE(3) group as

$$\begin{aligned}\dot{\mathcal{X}} &= \mathcal{X}\xi^\wedge, \\ \dot{\xi} &= J_b^{-1} \left(\text{ad}_\xi^* J_b \xi + u \right)\end{aligned}\quad (42)$$

The linearized twist dynamics are [14]:

$$\dot{\xi} = \Gamma_t \xi + \Lambda_t u + \mathbf{b}_t \quad (43)$$

where Γ_t , Λ_t and \mathbf{b}_t are:

$$\begin{aligned}\Gamma_t &:= J_b^{-1} \text{ad}_\xi^* J_b + J_b^{-1} \begin{bmatrix} (\mathbb{I}_b \omega)^\wedge & m v^\wedge \\ m v^\wedge & 0 \end{bmatrix} \\ \Lambda_t &:= J_b^{-1} \\ \mathbf{b}_t &:= -J_b^{-1} \begin{bmatrix} (\mathbb{I}_b \omega)^\wedge & m v^\wedge \\ m v^\wedge & 0 \end{bmatrix} \xi\end{aligned}\quad (44)$$

assuming the inertia matrix J_b is defined as

$$J_b := \begin{bmatrix} \mathbb{I}_b & 0 \\ 0 & m I_3 \end{bmatrix} \quad (45)$$

where \mathbb{I}_b and m are the moment of inertia in the body frame and the body mass, respectively.

B. Simulations

We evaluate the performance of our algorithm under the presence of generic nonlinear constraints, including unsafe configurations and obstacles. Moreover, we evaluate its effectiveness in handling external disturbances and compare its computational efficiency against a standard constrained SQP method.

1) *Constraint Handling*: We now test the proposed algorithm for planning a safe path for a SE(3) rigid body. The task we have defined involves rotating the body to the configuration $R_z(180)$ from the identity and translating it to the position (1, 1, 1) from the initial position (0, 0, 0) in 3 seconds with a fixed time step of $\Delta t=0.01$. To denote the rotation around the x , y , and z -axes of the body-fixed frame, we use $R_x(\cdot)$, $R_y(\cdot)$,

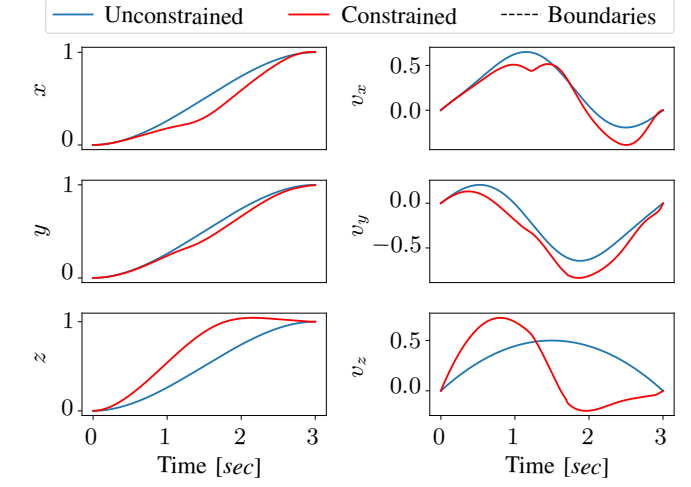


Fig. 4. Control inputs obtained by constrained and unconstrained DDP.

and $R_z(\cdot)$, respectively. During the motion, the configuration $R_z(90)$ is considered to be unsafe and must be avoided. Moreover, it is presumed that there are spherical obstacles situated at (0.55, 0.55, 0.5), (0.1, 0.0, 0.75), (0.5, 0.1, 0.1), and (0.1, 0.5, 0.1) with respective radii of 0.5, 0.25, 0.2, and 0.3, which must be evaded as well (Fig. 2). As the configuration avoidance constraints are incorporated based on the formulation presented in (22), an additional constraint is introduced for angular velocities with a bound of 1.4, following the description in (19).

To prioritize penalizing the final state and control inputs over the running states, we set the controller parameters as: $S_V=100I_{12}$, $S_U=0.001I_6$, and $S_Q=0.00005I_{12}$. In order to assess the performance of the proposed DDP in terms of constraint handling, we conducted an experiment with the same trajectory optimization task in both constrained and unconstrained cases, and the resulting state and control input trajectories are depicted in Fig. 3 and Fig. 4, respectively.

The configuration trajectories were converted to Euler angles (ϕ, θ, ψ in degrees) using the rotation order $R_x(\cdot)R_y(\cdot)R_z(\cdot)$. In the unconstrained case, it is shown that the ψ angle goes directly from 0 to 180 degrees while the ϕ

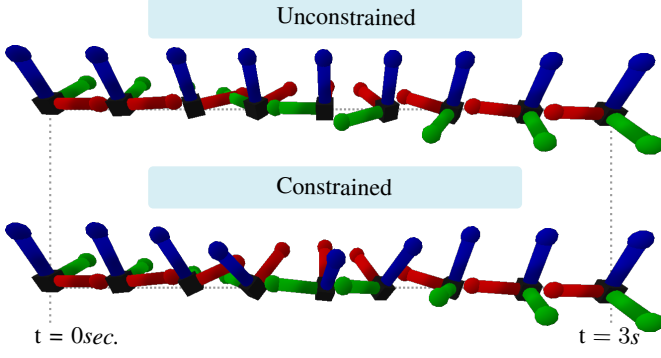


Fig. 5. Comparison of orientation trajectories generated by constrained and unconstrained DDP for an SE(3) object. Notably, when the configuration constraint is considered, the object begins to move along an alternate axis in order to circumvent the unsafe orientation.

and θ angles remain constant (Fig. 3), as the task only involves rotating around the z -axis. This can also be observed in the control inputs u_τ in Fig. 4, where only a single input is non-zero to achieve the desired motion, while the others remain zero. However, in the constrained case, rotations around x and y -axes (changes in ϕ and θ angles) were also observed to avoid the unsafe configuration of $R_x(90)$ (Fig. 3). When accounting for the configuration constraint, the object commences motion along different axes to bypass the unsafe orientation, as further illustrated in Fig. 5.

In the unconstrained case, the shortest paths for positional states were achieved (Fig. 3). However, the presence of four spherical obstacles necessitated adopting a more circuitous route, deviating along each axis to obtain a collision-free trajectory (Fig. 2). Apart from the configuration constraints concerning position and orientation, the constrained DDP satisfies the angular velocity bound of 1.4, whereas the ω_z value exceeds the bound in the unconstrained scenario.

2) *Disturbance Rejection*: To evaluate the effectiveness of the proposed DDP method in handling external disturbances, we extend the analysis done in [13] to SE(3) and employ the proposed DDP method as a Lie-algebraic feedback control:

$$u_k^{fb} := u_k^* + \mathbf{K}_k \log_m((\mathcal{X}_k^*)^{-1} \mathcal{X}_k^\epsilon) \quad (46)$$

where u_k^* and \mathbf{K}_k represent the (sub)optimal control sequence and time-varying feedback gains, respectively, which are obtained through DDP. The feed-forward term d_k in (31) is not explicitly shown in the feedback policy (46) because it is already included in u_k^* . The variables \mathcal{X}_k^* and \mathcal{X}_k^ϵ represent the (sub)optimal states obtained through DDP and the perturbed states due to disturbance, respectively.

We test the policy (46) on the following stochastic version of the SE(3) dynamics:

$$\begin{aligned} \mathcal{X}_{k+1}^\epsilon &= \mathcal{X}_k^\epsilon \exp_{m_{SE(3)}}(\xi_k^\epsilon \Delta t) \\ \xi_{k+1}^\epsilon &= \xi_k^\epsilon + f(\xi_k^\epsilon, u_k) \Delta t + \sigma_w w \end{aligned} \quad (47)$$

where w is assumed to be spatially uncorrelated independent and identically distributed noise, drawn from a zero mean Gaussian distribution, $w \sim \mathcal{N}(0_{6 \times 1}, I_6)$, $\sigma_w = 0.001$. The

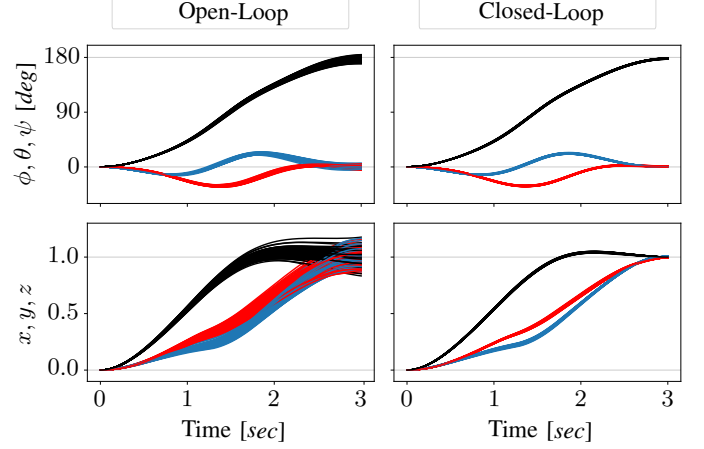


Fig. 6. The implementation of Lie-algebraic feedback control in the proposed DDP method notably reduces state variance, especially in the vicinity of goal points, when subjected to random disturbances.

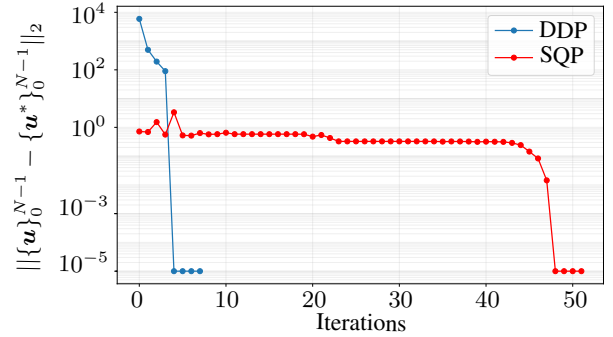


Fig. 7. Convergence comparison between standard constrained SQP and proposed constrained DDP methods, showcasing the significantly faster convergence achieved by DDP.

performance of the proposed DDP method under stochastic conditions was evaluated by allowing the optimizer to converge on the deterministic system and then testing its performance on the stochastic system. Fig. 6 shows the results of this comparison, using 1000 sampled trajectories under noisy dynamics to compare the open-loop policy u_k^* with the feedback policy u_k^{fb} (46). The results demonstrate that the use of the obtained feedback gains significantly reduces state variance, particularly in the vicinity of the goal points, as expected.

3) *Computational Efficiency*: A widely used approach to solving discrete optimal control problems involves utilizing readily available optimization solvers, which can be seamlessly applied with minimal modifications. Generating feasible trajectories can be achieved by treating the system dynamics as equality constraints and formulating both configuration and velocity constraints as inequality constraints.

In order to establish a benchmark comparison, we employed a Python optimizer that uses the Sequential Least Squares Programming (SLSQP) Algorithm [31], from the SciPy Optimization module. The task described in Section 3.2 proved challenging for a standard constrained SQP, as it involves

300 discrete steps with nonlinear equality and inequality constraints at each step. As a result, we tested a relatively simpler task: rotating the body from its identity configuration to $R_z(90)$ and translating it from the initial position $(0, 0, 0)$ to $(1, 1, 1)$ in 30 discrete steps, while avoiding a spherical obstacle with a 0.6 radius located at $(0.5, 0.5, 0.5)$. To accelerate convergence, we supplied derivative information for the cost function as well as equality and inequality constraints.

Figure 7 illustrates a comparison of convergence between the standard constrained SQP and the proposed constrained DDP methods. DDP achieves convergence in just 5 iterations, whereas SQP requires 47 iterations. The primary reason for this difference is that direct optimization methods increase the number of decision variables as the horizon expands, leading to a search in a space with numerous equality and inequality constraints. This result is consistent with the analysis presented in [13] regarding unconstrained DDP on Lie groups.

VII. CONCLUSION

In conclusion, the optimization of control policies on matrix Lie groups is an important problem in control and robotics with numerous applications. In this work, we have proposed a novel approach for tackling this problem using an augmented Lagrangian based constrained discrete DDP algorithm. Our method involves lifting the optimization problem to the Lie algebra in the backward pass, allowing us to compute the gradient of the objective and constraint functions within the corresponding tangent space. In the forward pass, we retract back to the manifold by integrating the dynamics using the optimal policy obtained in the backward pass.

A key contribution of our work is the development of a general approach for nonlinear constraint handling for a wide range of matrix Lie groups. Previous methods were only able to handle constraints for specific classes of matrix Lie groups, such as $SO(3)$ constraints. Our method, on the other hand, is able to handle a wide range of nonlinear constraints, making it a more widely applicable and flexible solution.

In addition, we have demonstrated the effectiveness of the method in handling external disturbances through its application as a Lie-algebraic feedback control policy on $SE(3)$. The results show that the approach is able to effectively handle constraints and maintain its stability in the presence of external disturbances.

Overall, the proposed DDP algorithm represents a significant step forward in the field of optimization on matrix Lie groups. It provides a flexible and general approach for nonlinear constraint handling and has the potential to be applied to a wide range of control problems.

In future research, exploring closed-loop uncertainty propagation throughout the prediction horizon, as demonstrated for Euclidean models in [26], could pave the way for a robust MPC framework tailored to matrix Lie groups. This advancement would enable the proposed method to operate effectively in more complex and dynamic environments.

REFERENCES

- [1] E. G. Hemingway and O. M. O'Reilly, "Perspectives on Euler angle singularities, gimbal lock, and the orthogonality of applied forces and applied moments." *Multibody System Dynamics*, 44, 31–56, 2018.
- [2] M. D. Shuster, "A survey of attitude representations." *Navigation*, 8(9), 439–517, 1993.
- [3] J. Diebel, "Representing attitude: Euler angles, unit quaternions, and rotation vectors." *Matrix*, 58(15-16), 1–35, 2006.
- [4] A.M. Bloch, *Nonholonomic Mechanics and Control*, Springer, 2015.
- [5] K. M. Lynch and F. C. Park, *Modern robotics*, Cambridge University Press, 2017.
- [6] F. Bullo and R. M. Murray, "Tracking for fully actuated mechanical systems: a geometric framework," *Automatica*, 35(1), 17–34, 1999.
- [7] F. Bullo and A. D. Lewis, *Geometric Control of Mechanical Systems: Modeling, Analysis, and Design for Simple Mechanical Control Systems*, Springer, 2019.
- [8] A. M. Bloch, I. I. Hussein, M. Leok, and A. K. Sanyal, "Geometric structure-preserving optimal control of a rigid body." *Journal of Dynamical and Control Systems*, 15(3), 307–330, 2009.
- [9] M. B. Kobilarov and J. E. Marsden, "Discrete Geometric Optimal Control on Lie Groups," *IEEE Transactions on Robotics*, 27(4), 641–655, 2011.
- [10] M. Kobilarov, M. Desbrun, J. E. Marsden, and G. S. Sukhatme, "A discrete geometric optimal control framework for systems with symmetries," *Robotics: Science and Systems*, 161–168, 2008.
- [11] S. Patil, J. Pan, P. Abbeel and K. Goldberg, "Planning Curvature and Torsion Constrained Ribbons in 3D With Application to Intracavitary Brachytherapy," *IEEE Transactions on Automation Science and Engineering*, 12(4), 1332–1345, 2015.
- [12] M. Kobilarov, "Discrete Optimal Control on Lie Groups and Applications to Robotic Vehicles," *IEEE International Conference on Robotics and Automation*, 5523–5529, 2014.
- [13] G.I. Boutselis, E. Theodorou, "Discrete-time differential dynamic programming on lie groups: Derivation, convergence analysis, and numerical results." *IEEE Transactions on Automatic Control*, 66(10), 4636–4651, 2020.
- [14] S. Teng, D. Chen, W. Clark and M. Ghaffari, "An Error-State Model Predictive Control on Connected Matrix Lie Groups for Legged Robot Control," *IEEE/RSJ International Conference on Intelligent Robots and Systems*, 8850–8857, 2022.
- [15] S. Teng, W. Clark, A. Bloch, R. Vasudevan and M. Ghaffari, "Lie Algebraic Cost Function Design for Control on Lie Groups," *IEEE Conference on Decision and Control*, 1867–1874, 2022.
- [16] S. Liu, and D. Liu, "Discrete-Time Differential Dynamic Programming on $SO(3)$ With Pose Constraints." *IEEE Access*, 10, 112921–112933, 2022.
- [17] T. Lee, "Geometric Tracking Control of the Attitude Dynamics of a Rigid Body on $SO(3)$." *IEEE American Control Conference*, 1200–1205, 2011.
- [18] T. Lee, M. Leok and N. H. McClamroch, "Geometric Tracking Control of a Quadrotor UAV on $SE(3)$," *IEEE Conference on Decision and Control*, 5420–5425, 2010.
- [19] A. Saccon, J. Hauser and A. P. Aguiar, "Optimal Control on Lie Groups: The Projection Operator Approach," *IEEE Transactions on Automatic Control*, 58(9), 2230–2245, 2013.
- [20] D. Y. Lee, R. Gupta, U. V. Kalabic, S. Di Cairano, A. M. Bloch, J. W. Cutler and I. V. Kolmanovsky, "Geometric mechanics based nonlinear model predictive spacecraft attitude control with reaction wheels," *Journal of Guidance, Control, and Dynamics*, 40(2), 309–319, 2017.
- [21] S. Hong, J. H. Kim and H. W. Park, "Real-Time Constrained Nonlinear Model Predictive Control on $SO(3)$ for Dynamic Legged Locomotion," *IEEE/RSJ International Conference on Intelligent Robots and Systems*, 3982–3989, 2020.
- [22] U. Kalabic, R. Gupta, S. Di Cairano, A. Bloch and I. Kolmanovsky, "MPC on manifolds with an application to $SE(3)$," *IEEE American Control Conference*, 7–12, 2016.
- [23] Y. Ding, A. Pandala, C. Li, Y. H. Shin and H. W. Park, "Representation-Free Model Predictive Control for Dynamic Motions in Quadrupeds," *IEEE Transactions on Robotics*, 37(4), 1154–1171, 2021.
- [24] M. Watterson, S. Liu, K. Sun, T. Smith and V. Kumar, "Trajectory optimization on manifolds with applications to quadrotor systems," *The International Journal of Robotics Research*, 39(2-3), 303–320, 2020.
- [25] D. H. Jacobson and D. Q. Mayne, "Differential Dynamic Programming." New York, NY, USA: Elsevier, 1970.
- [26] G. Alcan and V. Kyrki, "Differential Dynamic Programming With Non-linear Safety Constraints Under System Uncertainties," *IEEE Robotics and Automation Letters*, 7(2), 1760–1767, 2022.
- [27] M. Kobilarov, D.N. Ta, and F. Dellaert, "Differential Dynamic Programming for Optimal Estimation," *IEEE International Conference on Robotics and Automation*, 863–869, 2015.

- [28] A. Bloch, P. S. Krishnaprasad, J. E. Marsden, and T. S. Ratiu, “The Euler-Poincaré equations and double bracket dissipation,” *Communications in Mathematical Physics*, 175(1), 1—42, 1996.
- [29] T. A. Howell, B. E. Jackson and Z. Manchester, “ALTRO: A Fast Solver for Constrained Trajectory Optimization,” *IEEE/RSJ International Conference on Intelligent Robots and Systems*, 7674–7679, 2019.
- [30] M. Ghaffari, R. Zhang, M. Zhu, C. E. Lin, T. Y. Lin, S. Teng and J. Song, “Progress in Symmetry Preserving Robot Perception and Control Through Geometry and Learning.” *Frontiers in Robotics and AI*, 9, 2022.
- [31] D. Kraft, “A Software Package for Sequential Quadratic Programming.” *Forschungsbericht- Deutsche Forschungs- und Versuchsanstalt für Luft- und Raumfahrt*, 1988.